Electrocatalytic Performance of Interfacially Synthesized Au–Polyindole Composite toward Formic Acid Oxidation

ARTICLE *in* INDUSTRIAL & ENGINEERING CHEMISTRY RESEARCH · JUNE 2013

Impact Factor: 2.59 · DOI: 10.1021/ie400915s

3 AUTHORS, INCLUDING:

Ashish Kumar
Indian Institute of Technology (Banaras Hindu…
7 PUBLICATIONS **33** CITATIONS
SEE PROFILE

Rajiv Prakash
Indian Institute of Technology (Banaras Hindu…
135 PUBLICATIONS **1,353** CITATIONS
SEE PROFILE

I&EC research
Industrial & Engineering Chemistry Research

Article

pubs.acs.org/IECR

Electrocatalytic Performance of Interfacially Synthesized Au-Polyindole Composite toward Formic Acid Oxidation

Ashish Kumar, Leela Joshi, and Rajiv Prakash*

School of Materials Science and Technology, Indian Institute of Technology, Banaras Hindu University, Varanasi-221005, India

ABSTRACT: The current study proposes a composite having a Au cluster embedded within polyindole flakes (Au@Pin) as a promising electrocatalyst in formic acid oxidation. The present work provides a detailed study of the Au@Pin composite and its catalytic properties compared to those of a Au commercial electrode for oxidation of formic acid and a possible mechanism. The role of a morphology controlled composite and interaction of Au in the cages of polymers flakes are discussed for effective catalytic action of the material. The electrocatalytic oxidation of formic acid is carried out over a Au@Pin composite modified glassy carbon (GC) electrode. Voltammetric and chronoamperometric measurements show that a Au@Pin composite has better CO tolerance capability than Pin modified, bare GC and Au commercial electrodes. Electrochemical impedance spectroscopy (EIS) reveals consistent results and charge transfer mainly through a diffusion controlled process. On the basis of this EIS data, an equivalent electrical circuit is proposed. The higher catalytic activity of a Au@Pin composite toward formic acid oxidation in a mixture of 1.0 M HCOOH + 0.5 M H_2SO_4 electrolyte is observed in comparison to Pin modified and Au commercial electrodes due to the synergic effect between the Au cluster and Pin.

1. INTRODUCTION

Two major drawbacks of methanol as fuel in direct methanol fuel cells limit its usage in fuel cell applications. These drawbacks are (a) sluggish methanol oxidation over the anode and (b) methanol crossover through the polymer membrane.[1,2] Therefore, formic acid (FA) as fuel has been replacing methanol nowadays, because of its environmentally friendly nature and low costs in its diluted form.[3−5] It has been reported that the electrocatalytic oxidation of FA proceeds through three mechanisms. Initially it starts with adsorption of formic acid first; then these adsorbents either directly oxidize to carbon dioxide (called the *direct pathway*) or dehydrogenate to a bridge-adsorbed formate (called the *formate pathway*) or undergo dehydration to adsorbed carbon monoxide (called the *indirect pathway*) as shown earlier.[6]

The electrocatalytic performances of FA have been catalyzed by various catalysts. Among these metal based composite materials are state-of-the-art catalysts for promoting the oxidation of FA in electrochemical devices. In this context, several groups are studying the mechanisms of oxidation[7−11] using bimetals (e.g., Cu/Pd, Co/Pd, Pt/Cu, Pd/Au, etc.),[12−15] metal supported carbon (fiber or sheet),[16−18] and metal/polymer composites (e.g., Pd/polypyrrole, Au/polyaniline, Pt/polyindole, etc.) supported with carbon as electrode materials.[7,11,19] Mainly, their aim is to use these kinds of catalyst materials as anode in direct formic acid fuel cell application.

In view of size, generally nanometer scale metallic clusters have attracted considerable attention from past years. This is due to the superior functional properties of nanometallic clusters even in their small amount compared to bulk form in various fields such as catalysis, electronic application, or sensors.[20−24] Among various nanometallics, nano-gold cluster are one of the most inert elements used for heterogeneous catalyst both in industries as well as in laboratories. However, the rising price of gold has aroused a critical problem of cost prior to their large scale usage. So dispersion of these clusters with a conducting matrix is one of the choices to reduce this issue.

Heterocyclic conducting polymers are an excellent conducting matrix for the dispersion purpose of nanometallics because of good stability and participation of the heteroatom during redox performance as well as capability to hold nanoclusters within the matrix.[25,26] Among heterocyclic conducting polymers, polyindole (Pin) has attracted considerable interest due to the combinational property of both poly(*p*-phenylene) and polypyrrole together with fairly good thermal stability, redox property, slow degradation, and better air stability.[27−29]

Up to now, the nanocomposite of gold with polymers such as polypyrrole, polyaniline, polythiophene, polycarbazole, and polyindole has been synthesized by chemical and electrochemical techniques.[30−36] In these systems gold acts as a promoter for various applications such as catalysis, sensor, memory devices, and electronic applications due to a synergic effect between constituents of the nanocomposite.[37−40] However, there is no work reporting on the electro-oxidation of FA on a Au@Pin composite. In view of the above, we tried to explain the electrocatalytic FA oxidation by a Au@Pin nanocomposite and compared with Pin alone (formed by the interfacial polymerization method) and a Au commercial electrode. The experimentations were done on Au@Pin modified GC and Pin modified GC electrodes using differential pulse voltammetry (DPV), cyclic voltammetry (CV), electrochemical impedance spectroscopy (EIS), and chronoamperometry (CA). Prior to these analyses, the Au@Pin composite was thoroughly characterized by spectroscopy (XRD), X-ray photon spectroscopy (XPS), scanning electron microscopy

Received: March 21, 2013
Revised: June 2, 2013
Accepted: June 11, 2013
Published: June 11, 2013

dx.doi.org/10.1021/ie400915s | *Ind. Eng. Chem. Res.* 2013, 52, 9374−9380

(SEM), and transmission electron microscopy (TEM). The experimental analyses showed that the modified composite electrode exhibits excellent electrocatalysis toward FA oxidation due to a synergic effect between Au and polyindole, with the result indicating the possibility to employ this as a catalyst in the FA based fuel cells.

2. EXPERIMENTAL SECTION

2.1. Materials. Indole and hydrochloric acid were obtained from Merck, India. Chloroauric acid ($HAuCl_4$) was obtained from SRL, Sisco India Ltd. Ammonium peroxosulphate (APS) was obtained from Hi Media, India. All other chemicals used were of analytical grade. Double distilled water was used in all the experiments.

2.2. Synthesis of Au@ Pin Composite. In the synthesis scheme, an interfacial polymerization method was used in which a Au@ Pin composite was grown at the interface of two immiscible liquids. Two solutions, viz. nonaqueous (say solution A) and aqueous (say solution B), were prepared. Solution A was prepared by dissolving 100 mg of indole monomer in 10 mL of dichloromethane. Solution B was prepared by dissolving 314 mg of $HAuCl_4$ in 10.0 mL of (0.5 M) HCl, keeping the indole monomer to $HAuCl_4$ molar ratio as 1:1. Solution B was added slowly to solution A, resulting in the formation two distinct layers of solution B (top) and solution A (bottom) phases, which was further kept for 24 h for complete polymerization. After complete polymerization, dark-green Au@ Pin composite formed at the interface, which was separated and washed with distilled water followed by 0.2 M HCl. Au@ Pin composite was vacuum-dried at 50 °C and preserved for further experimentation.

Pin is synthesized by a similar technique for comparison purposes. In this technique, APS was taken in place of $HAuCl_4$. However, other parameters remained similar.

2.3. Electrode Fabrication. The typical modification of a GC electrode (of diameter 3 mm) by a Au@ Pin composite film on its surface was performed as follows: 0.5 mg of a Au@ Pin powdered composite material was mixed in 500 μL of THF and dispersed using ultrasonication for 10 min. Then 5 μL of this suspension was pipetted onto the surface of a freshly polished GC electrode. For comparison purposes, a Pin (synthesized from APS) modified GC electrode was also prepared in the same manner.

2.4. Instrumentation. A Au@Pin composite was analyzed for its structural properties and electrochemical oxidation of FA using various characterization techniques as follows: X-ray diffraction (XRD) analysis was performed on a Rigaku diffractometer using Cu Kα radiation with a wavelength of 1.54 Å. X-ray photoelectron spectroscopy (XPS) was performed with an AMICUS, U.K., instrument. Scanning electron microscopy (SEM) was performed on a Curl Zeiss, Supra-40 (Germany) instrument at the operating voltage 20 kV for the morphological analysis. Prior to experimentation, the sample was dispersed in tetrahydrofuran using ultrasonication and a drop was deposited onto a stab holding carbon tape. Transmission electron microscopy (TEM) was performed with an FEI Tecnai $30G^2S$-Twin electron microscope (USA) at an operating voltage of 300 kV. The samples were diluted in ethanol, and a drop was deposited onto a carbon-coated grid. Thermogravimetric analysis (TGA) was performed on a METTLER TULDEO, TGA/DSC 1 STARe System (Switzerland) at the rate of 10 °C min^{-1} in a nitrogen atmosphere.

Cyclic voltammetry (CV), differential pulse voltammetry (DPV), electrochemical impedance spectroscopy (EIS), and chronoamperometry (CA) were performed on a CH-Instrument Electrochemical Workstation (Model 7401; TX, USA) and Metrohm Autolab (PGSTAT-12/30/302; The Netherlands), respectively, using a three-electrode system. In this technique Ag/AgCl as reference, Pt-plate as counter, and glassy carbon modified by Au@ Pin composite and Pin as working electrodes were used to investigate the FA oxidation in a mixture of 1.0 M HCOOH + 0.5 M H_2SO_4 as electrolyte.

3. RESULTS AND DISCUSSION

In our previous work we have shown that the morphology of the polymers or polymer composites can be controlled during the synthesis by changing the synthesis methods or conditions.[36,41,42] It is already reported that the interfacial polymerization is a unique method for morphology control and obtaining various morphologies as rods, tubes, and spheres by changing the synthesis conditions and molar ratios of oxidant and monomer.[41,42] This time we observed a flake-type texture (as discussed later) during the interfacial synthesis using a different molar ratio of oxidant and monomer. The encapsulation of metals (such as Pt, Au, etc.) within a polymer matrix having an electron rich moiety enhances the overall performances of resulting composites. This is due to the synergic effect between metal clusters and the electron rich center of polymers such as polyindole, polyaniline, polycarbazole, or macrocyclic compounds.[35,38,39] In view of this concept, the Au@Pin composite and Pin are characterized by various tools and compared for electrocatalytic oxidation of FA with a Au commercial electrode. The various characterizations and comparisons are described below one by one.

3.1. Structural Properties. *3.1.1. XRD Analysis.* The XRD pattern of a Au@Pin composite exhibits the existence of reduced Au within the Pin matrix. Highly intense peaks (four peaks) are observed for reduced Au crystal planes (as shown in Figure 1) while less intense peaks (two peaks) are for Pin

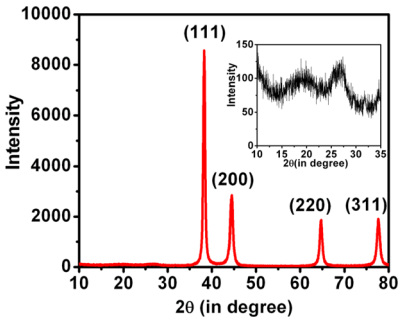

Figure 1. XRD pattern of the Au@Pin composite. Inset shows the zoom form of the pattern from 2θ = 10−35.

(as shown in inset), similar to earlier reports. This is due to the highly scattering nature of metals compared to polymer.[43] Four intense peaks at 38.4, 44.5, 64.7, and 77.8 are seen corresponding to the (111), (200), (220), and (311) planes of FCC gold, respectively, while the two peaks at 19.5 and 26.8 are due to the semicrystalline characteristics of Pin.[44]

3.1.2. XPS Analysis. The chemical analysis of the Au@Pin composite was done by XPS for Au (4f), N (1s), and C (1s) as shown in Figure 2. Figure 2a shows the multiplet spectrum for the typical high resolution core-level Au (4f). The first doublet peak observed corresponds to Au ($4f_{7/2}$) and Au ($4f_{5/2}$), with

dx.doi.org/10.1021/ie400915s | Ind. Eng. Chem. Res. 2013, 52, 9374−9380

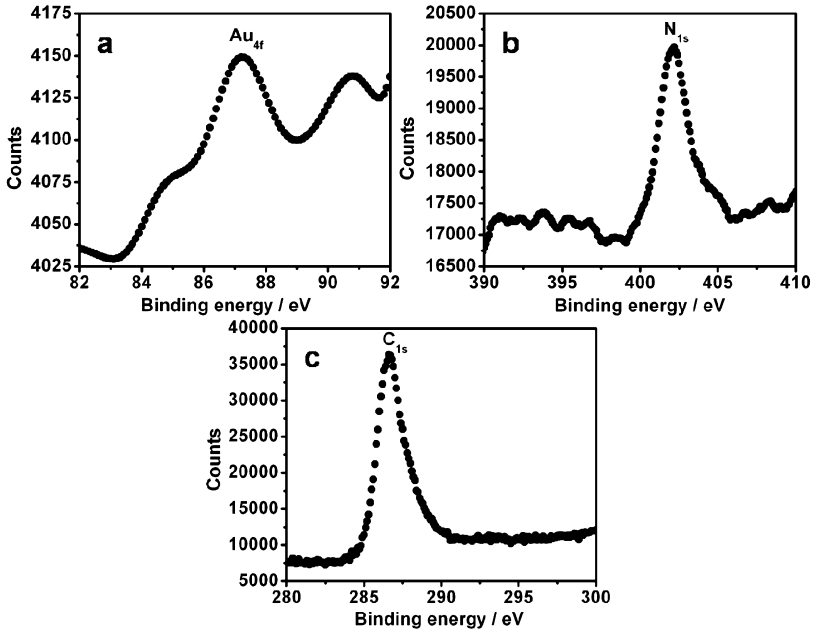

Figure 2. XPS curves of elements Au (4f), N (1s), and C (1s) on a glass substrate for the Au@Pin composite.

binding energies of 84.8 and 87.2 eV, respectively, which are typical values for Au (0) species,[45] while the second doublet peak at binding energies 87.2 ($4f_{7/2}$) and 90.7 ($4f_{5/2}$) corresponds to Au (+III) species as contaminant.[46]

Similarly, parts b and c of Figure 2 show the typical high resolution core-level N (1s) and C (1s) spectra of the composite at 402 and 286.6 eV, respectively. The appearance of these peaks was an indication of Pin in the Au@Pin composite similar to polyaniline.[47]

3.1.3. SEM Analysis. The morphological texture of the Au@Pin composite was investigated by SEM as shown in Figure 3a. The composite possesses a highly porous texture in which nearly spherical Au clusters get associated within Pin flakes (*cf.* from inset). This type of morphology may be expected due to interaction of reduced Au clusters (obtained from oxidant during polymerization) with polymer at the interface of the solvents. The spherical shape of a Au cluster within the polymer background (shaded portion in Figure 3b) was also observed by TEM micrograph. The presence of Au clusters was cross-checked, and their crystal plane within the polymer was reinvestigated through a selected area diffraction pattern (SADP) taken over the spherical region by TEM as shown in Figure 3c. Various crystal planes of Au clusters were identified and indexed to (111), (200), (220), and (311) crystalline facets, which is consistent to XRD.

3.1.4. Thermal Analysis. The approximate amount of Au in the Au@Pin composite was obtained by TGA performed in inert atmosphere as shown in Figure 4. In this technique, the same amount of Au@Pin and Pin alone are heated under similar experimental conditions (*cf.* (Figure 4) up to the temperature of complete decomposition of Pin. On the basis of the remaining amount of residue, it was calculated that the Au is present 41% (by weight) in the Au@Pin composite (difference of curve a and b at 800 °C).

3.2. Electrocatalytic Property. Developing a catalyst electrode toward FA oxidation is one of the major tasks of this paper for application in fuel cell areas. The catalytic performance of the Au@Pin composite and Pin (formed by APS) toward FA oxidation was investigated in a manner similar to

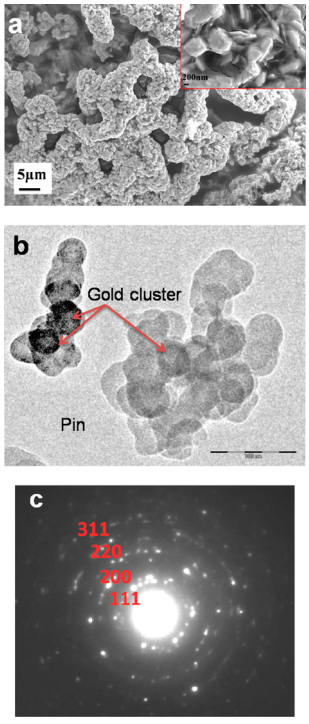

Figure 3. (a) SEM image of a Au@Pin composite. Inset shows enlarged view of SEM at higher magnification. (b) TEM image of a Au@Pin composite and (c) SADP of Au clusters obtained using TEM.

our earlier published work based on the SnO_2−Pin composite.[48] A GC electrode was modified with these catalytic materials and compared with a Au commercial electrode using DPV as shown in Figure 5.

On comparing both clusters, i.e. Au and SnO_2, Au clusters have long been studied as multifunctional materials compared to SnO_2 toward various catalytic applications. This is due to their more stable performance as catalyst or support catalyst compared to SnO_2, especially for a series of those catalytic reactions that is carried out in the presence of long exposure to an

dx.doi.org/10.1021/ie400915s | Ind. Eng. Chem. Res. 2013, 52, 9374−9380

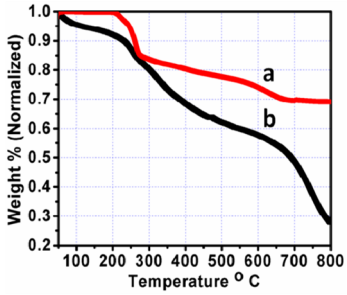

Figure 4. Thermogram of (a) Au@Pin and (b) Pin.

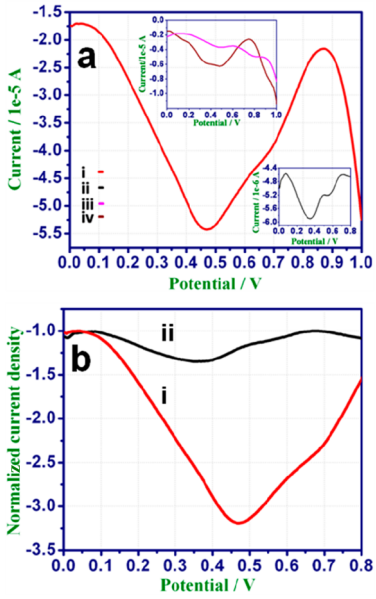

Figure 5. (a) DPV of FA oxidation for (i) Au@Pin composite modified, (ii) bare GC, (iii) Pin modified, and (iv) Au commercial electrode in 1.0 M HCOOH + 0.5 M H_2SO_4. (b) Normalized current density of (i) Au@Pin and (ii) SnO_2−Pin composites with electrochemical active surface area.

acidic environment.[49,50] However, slow degradation of SnO_2 particles occurs after long exposure to aqueous H_2SO_4, which limits their usage even after use as a support catalyst.[51] Herein we tried to show the influences of Au in Pin compared to SnO_2 in Pin. There are two well-defined peaks that are observed in which the first large anodic peak at 0.49 V is attributed to the direct oxidation of FA to CO_2, while the second small shoulder peak at 0.70 V is related to the oxidation of adsorbed intermediate CO species.[1,52] In a Au@Pin composite modified electrode (as shown in Figure 5a(i)), the voltammogram indicates suppression of the second shoulder peak at 0.70 V. This is due to the strong CO tolerance capability of the composite toward FA oxidation (vs Ag/AgCl). This phenomenon may be due to a synergic effect between a Au cluster and an electron rich center (means the available electron on the nitrogen moiety) of the Pin similar to that earlier reported[35,38,52] which retards the CO formation on the modified electrode surface. However, compared to a Au@Pin modified electrode, bare GC, Pin, and Au commercial electrodes (*cf.* Figure 5a(ii), a(iii), and a(iv)) follow both direct and indirect pathways. The normalized current density (by the electrochemical active surface area of modified GC electrodes) of the Au@Pin composite is compared with the SnO_2−Pin composite as shown in the Figure 5b. The electrochemical active surface areas of Au@Pin and SnO_2−Pin composites are calculated as 5.6 and 5.8 mm^2, respectively, by adopting a procedure reported earlier.[53] On comparing both DPV results (*cf.* Figure 5b(i) andb(ii)), the oxidation potentials for FA slightly shifted toward the higher side with relatively higher current density. This may be probably due to better interaction of Au clusters with Pin in Au@Pin compared to SnO_2 in SnO_2−Pin. To confirm the consistency of DPV results for as synthesized materials toward FA oxidation, CVs were performed in the same concentration of electrolytes as shown in Figure 6.

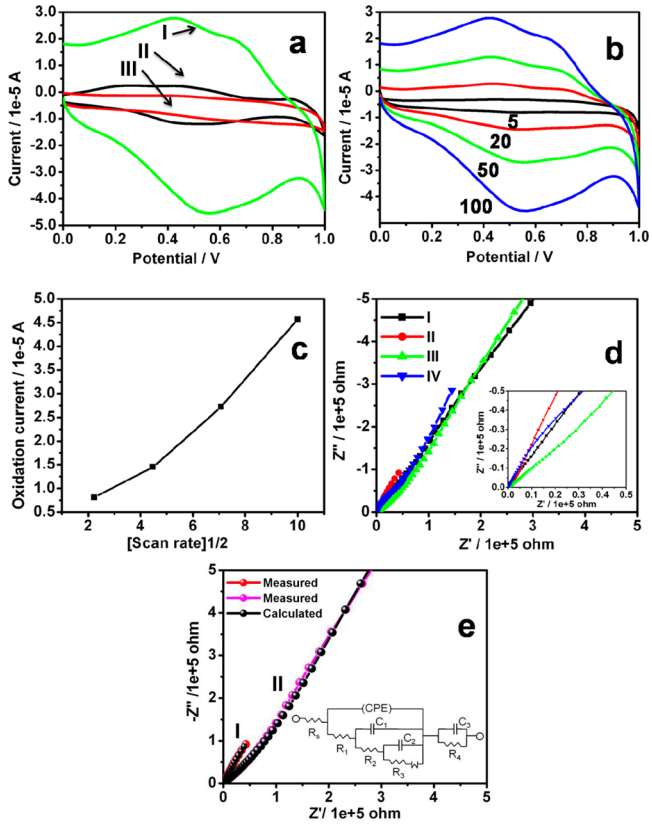

Figure 6. (a) CV of (i) Au@ Pin composite modified, (ii) Au commercial, and (iii) Pin modified electrodes at scan rate 100 mV/s; (b) CVs of Au@ Pin composite modified electrode at different scan rates from 5 to 100 mV/s; (c) oxidation peak current versus square root of scan rate at fixed concentration of FA using a Au@ Pin composite modified electrode; (d) EIS of (i) bare GC, (ii) Au@ Pin composite modified, (iii) Pin modified, and (iv) Au commercial electrode. Inset shows enlarged view of EIS and (e) EIS data fitted by ZSimp software for Au@Pin (i) and Pin (ii) with their electrical equivalent circuit (in inset).

It can be seen from the CV plot obtained at 100 mV/s that FA oxidation on a Au@ Pin composite modified electrode showed two anodic peaks (similar to DPV results) in the forward scan. However, a higher area under the voltammogram of this catalyst compared with a Pin modified and Au commercial electrode (*cf.* Figure 6a(i), a(ii), and a(iii)) is clear indication for accumulation of more charges near the electrode surface than with a Pin or Au commercial electrode. In order to check the stability of this prepared composite and their electrocatalytic properties at different scan rates toward FA oxidation in 1.0 M HCOOH + 0.5 M H_2SO_4, CV's were again performed

dx.doi.org/10.1021/ie400915s | *Ind. Eng. Chem. Res.* 2013, 52, 9374−9380

Table 1. Electrochemical Impedance Parameters Calculated from the Equivalent Circuit Model

material	R_s (Ω)	CPE (μS·s^n)	frequency power ($0 < n < 1$)	R_1 (Ω)	C_1 (μF)	R_2 (Ω)	C_2 (μF)	R_3 (Ω)	W (S·s$^{1/2}$)	C_3 (μF)	R_4 (Ω)	$\chi^2 \times 10^{-4}$
Au@Pin	12.46	45.3	0.68	5515	15.7	2.28 x10^{-4}	22.7	1.66 x10^{-6}	1.4 × 10^{-1}	4.66	4.1	7.7
Pin	18.27	5.6	0.47	3609	0.038	4460	0.04	16686	1.9 × 10^{-6}	2.0	2.34 x10^6	4.4

on a Au@ Pin modified electrode at different scanning rates (as shown in Figure 6b). With an increase in the scan rate, the oxidation peak currents enhance gradually, though the oxidation peak potentials are slightly positively shifted for about 28 mV. A linear relationship between the FA oxidation peak current and the square root of the scan rates (as shown in Figure 6c) is observed at fixed FA concentration, suggesting that the FA oxidation on this Au@Pin composite modified electrode is still dominated by a diffusion controlled process.[54,55] However, a slight positive deviation from the ideal behavior may likely be due to the fast charge transfer diffusion dominated process.[56,57] The diffusion controlled phenomenon in the Au@ Pin composite modified electrode was also observed during EIS measurement in terms of a Nyquist plot at its own open circuit potentials as shown in Figure 6d. In the general interpretation, the generation of a straight line (at low frequency or high $-Z''$) presents a diffusion controlled process while a semicircle (at high frequency or or low $-Z''$) represents resistance to charge transfer (R_{ct}).[55] However, the higher the inclination of the straight line part toward the $-Z''$ axis, the higher the charge accumulation near the electrode surface.[58] It can be seen from EIS results as shown in Figure 6d, except for the Au commercial electrode, that all modified GC electrodes (with Au@ Pin composite and Pin) and bare GC proceed through a diffusion controlled process while the inclination of curve (ii) compared to curve (i) and curve (iii) (as shown in the inset of Figure 6d) toward the $-Z''$ axis was a clear indication for the capability of more charge accumulation near the surface compared to bare GC and Pin.

The resulting EIS data is fitted (with the help of ZSimp Win software, Version-3.22) for the demonstration of electron transfer properties at the vicinity of modified Au @Pin compared to Pin electrodes and electrochemical parameters are evaluated corresponding to their equivalent circuit with chi-squared minimized 10^{-4} (chi square is the function defined as the sum of the squares of residuals) as shown in Figure 6e. We observed excellent agreement between experimental EIS results and the parameters calculated from the best fitting electrical equivalent circuit model [R(Q(R(C(R(C(RW))))))(CR)] (as shown in the inset of Figure 6e). The first one is the bulk solution resistance of the Au@Pin and the electrolyte, Rs; the second one is the parallel combination of the constant phase element, Q or CPE, and electrolyte resistance R_1 at the interface of the electrode for a few seconds; the third one is a parallel combination of double layer capacitance, C_1, and pore resistance, R_2.[59] Similarly, the fourth elements (parallel capacitance, C_2, with charge transfer resistance, R_3, which is in series with the Warburg element, W) are due to finite diffusion,[60] and the last component a capacitance, C_3, is introduced in parallel with a resistance, R_4, corresponding to the electrochemical phenomenon at the microelectrode surface after the diffusion of FA. The same circuit is adopted for Pin to evaluate the effect of gold in a Au@Pin composite, and the comparative electrochemical parameters are summarized in Table 1. On comparing both the calculated EIS parameter (after fitting) and the resistance of charge transfer, the R_3 value of the Au@Pin composite is relatively much lower compared to Pin while the contributions of W and C_2 are 1.4 × 10^{-1} S·s$^{-1/2}$ and 22.7 μF, respectively, in the case of the Au@Pin composite, which is higher than that of Pin. This means that the EIS phenomenon occurs mainly through a diffusion dominated process with higher accumulation of charge near the electrode due to contribution of Au in the Au@Pin composite.

For a feasible catalyst to possibly use, a Au@Pin composite modified GC electrode must exhibit stable and long-term activity toward FA oxidation compared to Pin modified GC, bare GC, and Au commercial electrode. Therefore, to compare their activities and current stability, a CA experiment (as shown in Figure 7) was performed initially within a potential range

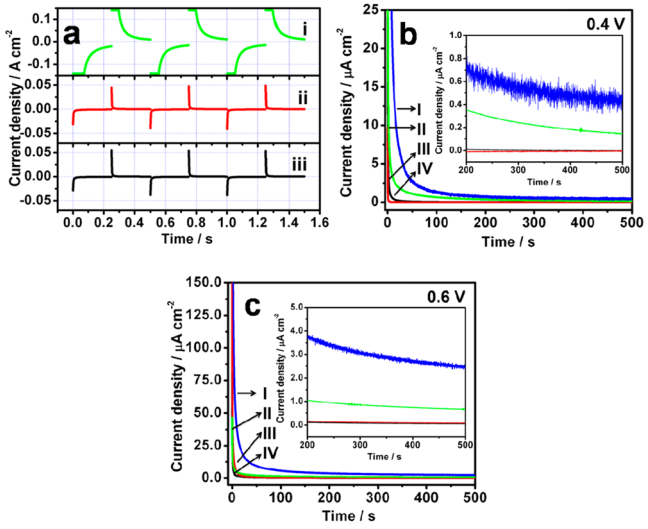

Figure 7. CA of (a) Au@Pin composite modified, pin modified, and Au commercial electrode (I, II, and III) within potentials from 0.0 to 1.0 V, (b) Au@Pin composite modified, Pin modified, Au commercial, and GC electrode (I, II, III, and IV) at 0.4 V, and (c) Au@Pin composite modified, Pin modified, Au commercial, and GC electrode (I, II, III, and IV) at 0.6 V in 1.0 M HCOOH + 0.5 M H_2SO_4.

(0−1 V) for a short time and then for a long time at 0.4 and 0.6 V in a mixture of 1.0 M HCOOH and 0.5 M H_2SO_4 with respect to Ag/AgCl electrode. Figure 7a presents the CA redox profile of modified electrodes (Au@Pin composite and Pin) and Au commercial electrode within the applied potential range 0−1 V for a short period of time. Initially the oxidation current density for the Au@Pin composite is 0.14 A cm^{-2}, whereas those for Pin and the Au commercial electrode are 0.045 and 0.056 A cm^{-2}, respectively. This is approximately a factor of 3 improvement over Pin and 2.5 improvement over Au commercial electrode. However, the symmetrical nature of the CA profile presents a more stable performance of the Au@Pin composite modified electrode toward FA oxidation.

Compared to Pin modified and Au commercial electrodes, a similar nature of the Au@Pin composite modified electrode was observed when CA performed at fixed potentials (0.4 and 0.6 V). The polarization current densities of Pin and bare GC and Au

dx.doi.org/10.1021/ie400915s | Ind. Eng. Chem. Res. 2013, 52, 9374−9380

commercial electrodes, compared to a Au@Pin composite modified electrode, at both 0.4 and 0.6 V (*cf.* Figure 7b-ii, iii, iv with Figure 7b-i, and Figure 6c-ii, iii, iv with Figure 7c-i,) decrease rapidly at the initial stage, which is due to the formation of double layer capacitance as well as accumulation of CO species over Pin.[61,62] At an applied potential of 0.6 V (*vs* Ag/AgCl), initially the Au@Pin composite modified electrode exhibits 251 μA cm^{-2}, which undergoes gradual degradation up to 2.48 μA cm^{-2} at 500 s. Similarly at 0.4 V, initially the current density is 149.0 and 0.42 μA cm^{-2} after 500 s. This is the highest current density difference compared to Pin modified and GC and Au commercial electrodes (at 0.4 and 0.6 V) or even a Au@Pin composite modified electrode (at 0.4 V), as summarized and shown in Table 2.

Table 2. Current Densities toward FA Oxidation of Catalysts (*vs* Ag/AgCl) during CA Analysis[a]

	current density (in μAcm^{-2})	
material	at 0.4 V	at 0.6 V
Au@Pin composite	149.0 (0.42)	251.0 (2.48)
Pin	66.8 (0.14)	55.8 (0.63)
Au commercial	9.67 (0.003)	149.5 (0.18)
GCE	62.4 (0.005)	105.16 (0.15)

[a]The number indicated inside parentheses represents current densities at 500 s.

4. CONCLUSION

A Au@Pin composite was successfully synthesized by an interfacial polymerization method and thoroughly characterized by XRD, XPS, SEM, and TEM. These characterization tools exemplify that nearly spherical reduced Au clusters get embedded within the flakes of Pin. The GC electrode was modified using a Au@Pin composite and demonstrated and compared for catalytic oxidation of FA (for fuel cell application) by DPV, CV, and CA measurements. It was observed that a Au@Pin composite modified GC electrode exhibits better CO tolerance capability with excellent activity and stability compared to Pin modified, bare GC and Au commercial electrodes. This is probably due to a synergic effect of nano Au-metal clusters and electron rich centers of Pin polymer and interaction of both the components. This work demonstrated a novel concept for insertion of metals within a cage of conducting polymers. The resulting composite may be considered as a cost-effective material that can replace the utilization of pure metal particles in some specific conditions for fuel cell technology or other applications.

AUTHOR INFORMATION

Corresponding Author

*E-mail: rajivprakash12@yahoo.com. Tel: +91-9935033011. Fax: +91-542-2368707.

Notes

The authors declare no competing financial interest.

ACKNOWLEDGMENTS

The authors would like to thank Prof. A. S. K. Sinha, HOD, Department of Chemical Engineering, Indian Institute of Technology (BHU), Varanasi, for providing the XPS facility.

REFERENCES

(1) Liu, F.; Lu, G.; Wang, C.-Y. Low crossover of methanol and water through thin membranes in direct methanol fuel cells. *J. Electrochem. Soc.* **2006**, *153*, A543−A553.

(2) Iwasita, T. Electrocatalysis of Methanol Oxidation. *Electrochim. Acta* **2002**, *47*, 3663−3674.

(3) Cheng, T. T.; Gyenge, E. L. Novel catalyst-support interaction for direct formic acid fuel cell anodes: Pd electrodeposition on surface-modified graphite felt. *J. Appl. Electrochem.* **2009**, *39*, 1925−1938.

(4) Liao, C.; Wei, Z. D.; Chen, S. G.; Li, L.; Ji, M. B.; Tan, Y.; Liao, M. J. Synergistic Effect of Polyaniline-Modified Pd/C Catalysts on Formic Acid Oxidation in a Weak Acid Medium $(NH_4)_2SO_4$. *J. Phys. Chem. C* **2009**, *113*, 5705−5710.

(5) Xu, W.; Gao, Y.; Lu, T.; Tang, Y.; Wu, B. Kinetic study of formic acid oxidation on highly dispersed carbon supported Pd−TiO_2 electrocatalyst. *Catal. Lett.* **2009**, *130*, 312−317.

(6) Chen, Y. X.; Heinen, M.; Jusys, Z.; Behm, R. J. Kinetics and Mechanism of the Electrooxidation of Formic Acid—Spectroelectrochemical Studies in a Flow Cell. *Angew. Chem., Int. Ed.* **2006**, *45*, 981−985.

(7) Ding, K.; Jia, H.; Wei, S.; Guo, Z. Electrocatalysis of Sandwich-structured Pd/Polypyrrole/Pd composites toward formic acid oxidation. *Ind. Eng. Chem. Res.* **2011**, *50*, 7077−7082.

(8) Zhang, S.; Shao, Y.; Yin, G.; Lin, Y. Electrostatic self-assembly of a Pt-around-Au nanocomposite with high activity towards formic acid oxidation. *Angew. Chem., Int. Ed.* **2010**, *49*, 2211−2214.

(9) Qu, K.; Wu, L.; Ren, J.; Qu, X. Natural DNA-modified graphene/Pd nanoparticles as highly active catalyst for formic acid electrooxidation and for the Suzuki reaction. *ACS Appl. Mater. Interfaces* **2012**, *4*, 5001−5009.

(10) Zhou, W.; Wang, C.; Xu, J.; Du, Y.; Yang, P. High efficient electrooxidation of formic acid at a novel Pt−indole composite catalyst prepared by electrochemical self-assembly. *J. Power Sources* **2011**, *196*, 1118−1122.

(11) Zhou, W.; Dua, Y.; Zhang, H.; Xu, J.; Yang, P. High efficient electrocatalytic oxidation of formic acid on Pt/polyindoles composite catalysts. *Electrochim. Acta* **2010**, *55*, 2911−2917.

(12) Zhao, H.; Yu, C.; You, H.; Yang, S.; Guo, Y.; Ding, B.; Song, X. A green chemical approach for preparation of Pt_xCu_y nanoparticles with a concave surface in molten salt for methanol and formic acid oxidation reactions. *J. Mater. Chem.* **2012**, *22*, 4780−4789.

(13) Bromberg, L.; Fayette, M.; Martens, B.; Luo, Z. P.; Wang, Y.; Xu, D.; Zhang, J.; Fang, J.; Dimitrov, N. Catalytic performance comparison of shape-dependent nanocrystals and oriented ultrathin films of Pt_4Cu alloy in the formic acid oxidation process. *Electrocatalysis* **2013**, *4*, 24−36.

(14) Mazumder, V.; Chi, M.; Mankin, M. N.; Liu, Y.; Metin, O.; Sun, D.; More, K. L.; Sun, S. A facile synthesis of MPd (M = Co, Cu) nanoparticles and their catalysis for formic acid oxidation. *Nano Lett.* **2012**, *12*, 1102−1106.

(15) Chen, G.; Liao, M.; Yu, B.; Li, Y.; Wang, D.; You, G.; Zhong, C. J.; Chen, B. H. Pt decorated PdAu/C nanocatalysts with ultralow Pt loading for formic acid electrooxidation. *Int. J. Hydrogen Energy* **2012**, *37*, 9959−9966.

(16) Morgan, R. D.; Salehi-khojin, A.; Masel, R. I. Superior formic acid oxidation using carbon nanotube-supported palladium catalysts. *J. Phys. Chem. C* **2011**, *115*, 19413−19418.

(17) Huang, H.; Wang, X. Pd nanoparticles supported on low-defect graphene sheets: for use as high-performance electrocatalysts for formic acid and methanol oxidation. *J. Mater. Chem.* **2012**, *22*, 22533−22541.

(18) Hu, G.; Nitze, F.; Barzegar, H. R.; Sharifi, T.; Mikołajczuk, A.; Tai, C. W.; Borodzinski, A.; Wagberg, T. Palladium nanocrystals supported on helical carbon nanofibers for highly efficient electrooxidation of formic acid, methanol and ethanol in alkaline electrolytes. *J. Power Sources* **2012**, *209*, 236−242.

(19) Pandey, R. K.; Lakshminarayanan, V. Electro-oxidation of formic acid, methanol, and ethanol on electrodeposited Pd-polyaniline nanofiber films in acidic and alkaline medium. *J. Phys. Chem. C* **2009**, *113*, 21596−21603.

(20) Zhou, Z. Y.; Ren, J.; Kang, X.; Song, Y.; Sun, S. G.; Chen, S. Butylphenyl-functionalized Pt nanoparticles as CO-resistant electrocatalysts for formic acid oxidation. *Phys. Chem. Chem. Phys.* **2012**, *14*, 1412−1417.

(21) Gu, X.; Lu, Z. H.; Jiang, H. L.; Akita, T.; Xu, Q. Synergistic catalysis of metal-organic framework-immobilized Au/Pd nanoparticles in dehydrogenation of formic acid for chemical hydrogen Storage. *J. Am. Chem. Soc.* **2011**, *133*, 11822−11825.
(22) Wu, G. H.; Wu, Y. F.; Liu, X. W.; Rong, M. C.; Chen, X. M.; Chen, X. An electrochemical ascorbic acid sensor based on palladium nanoparticles supported on graphene oxide. *Anal. Chim. Acta* **2012**, *745*, 33−37.
(23) Tan, E.; Yin, P.; Lang, X.; Wang, X.; You, T.; Guo, L. Functionalized gold nanoparticles as nanosensor for sensitive and selective detection of silver ions and silver nanoparticles by surface-enhanced Raman scattering. *Analyst* **2012**, *137*, 3925−3928.
(24) Ruffino, F.; Grimaldi, M. G.; Giannazzo, F.; Roccaforte, F.; Raineri, V. Size-dependent Schottky barrier height in self-assembled gold nanoparticles. *Appl. Phys. Lett.* **2006**, *89*, 243113−243116.
(25) Zhou, W.; Dua, Y.; Zhang, H.; Xu, J.; Yang, P. High efficient electrocatalytic oxidation of formic acid on Pt/polyindoles composite catalysts. *Electrochim. Acta* **2010**, *55*, 2911−2917.
(26) Zhou, W.; Xu, J.; Du, Y.; Yan, P. Polycarbazole as an efficient promoter for electrocatalytic oxidation of formic acid on Pt and PteRu nanoparticles. *Int. J. Hydro. Ener.* **2011**, *36*, 1903−1912.
(27) Billaud, D.; Maarouf, E. B.; Hannecart, E. Chemical oxidation and polymerization of indole. *Synth. Met.* **1995**, *69*, 571−572.
(28) Maarouf, E. B.; Billaud, D.; Hannecart, E. Electrochemical cycling and electrochromic properties of polyindole. *Mater. Res. Bull.* **1994**, *29*, 637−643.
(29) Zhijiang, C.; Guang, Y. Synthesis of polyindole and its evaluation for Li-ion battery applications. *Synth. Met.* **2010**, *160*, 1902−1905.
(30) Xue, K.; Xu, Y.; Song, W. One-step synthesis of 3D dendritic gold@polypyrrole nanocomposites via a simple self-assembly method and their electrocatalysis for H_2O_2. *Electrochim. Acta* **2012**, *60*, 71−77.
(31) Qiu, L.; Peng, Y.; Liu, B.; Lin, B.; Peng, Y.; Malik, M. J.; Yan, F. Polypyrrole nanotube-supported gold nanoparticles: An efficient electrocatalyst for oxygen reduction and catalytic reduction of 4-nitrophenol. *Appl. Catal., A* **2012**, *413− 414*, 230−237.
(32) Xu, X.; Liu, X.; Yu, Q.; Wang, W.; Xing, S. Architecture-adapted raspberry-like gold@polyaniline particles: facile synthesis and catalytic activity. *Colloid Polym. Sci.* **2012**, *290*, 1759−1764.
(33) Zhang, X.; Zhang, X.; Feng, R.; Liu, L.; Meng, H. Synthesis, characterization and catalytic activity of Au nanoparticles supported on PANI/a-Fe2O3 composite carriers. *Mater. Chem. Phys.* **2012**, *136*, 555−560.
(34) Tanaka, M.; Fujita, R.; Nishide, H. Coupling reaction on gold nanoparticle to yield polythiophene/gold nanoparticle alternate network film. *J. Nanosci. Nanotechnol.* **2009**, *9*, 634−639.
(35) Gupta, B.; Joshi, L.; Prakash, R. Novel synthesis of polycarbazole−gold nanocomposite. *Macromol. Chem. Phys.* **2011**, *212*, 1692−1699.
(36) Joshi, L.; Prakash, R. Polyindole-Au nanocomposite produced at the liquid/liquid interface. *Mater. Lett.* **2012**, *66*, 250−253.
(37) Cui, Y.; Chen, H.; Tang, D.; Yang, H.; Chen, G. Au(III)-promoted polyaniline gold nanospheres with electrocatalytic recycling of self-produced reactants for signal amplification. *Chem. Commun.* **2012**, *48*, 10307−10309.
(38) Li, Z. F.; Blum, F. D.; Bertino, M. F.; Kim, C. S. Amplified response and enhanced selectivity of metal-PANI fiber composite based vapor sensors. *Sens. Actuators, B* **2012**, *161*, 390−395.
(39) Baker, C. O.; Shedd, B.; Tseng, R. J.; Martinez-Morales, A. A.; Ozkan, C. S.; Ozkan, M.; Yang, Y.; Kaner, R. B. Size control of gold nanoparticles grown on polyaniline nanofibers for bistable memory devices. *ACS Nano* **2011**, *5*, 3469−3474.
(40) Raimondo, C.; Crivillers, N.; Reinders, F.; Sander, F.; Mayor, M.; Samori, P. Optically switchable organic field-effect transistors based on photoresponsive gold nanoparticles blended with poly(3-hexylthiophene). *Proc. Natl. Acad. Sci. U.S.A.* **2012**, *109*, 12375−12380.
(41) Gupta, B.; Prakash, R. Interfacial polymerization of carbazole: Morphology controlled synthesis. *Synth. Met.* **2010**, *160*, 523−528.
(42) Gupta, B.; Dhauhan, D. S.; Prakash, R. Controlled morphology of conducting polymers: Formation of nanorods and microspheres of polyindole. *Mater. Chem. Phys.* **2010**, *120*, 625−630.
(43) Feng, X.; Huang, H.; Ye, Q.; Zhu, J. J.; Hou, W. Ag/Polypyrrole Core-shell nanostructures: Interface polymerization, characterization and modification by gold nanoparticles. *J. Phys. Chem. C* **2007**, *111*, 8463−8468.
(44) Joshi, L.; Prakash, R. One-pot synthesis of Polyindole−Au nanocomposite and its nanoscale electrical properties. *Mater. Lett.* **2011**, *65*, 3016−3019.
(45) Casaletto, M. P.; Longo, A.; Martorana, A.; Prestianni, A.; Venezia, A. M. XPS study of supported gold catalysts: The role of Au^0 and $Au^{+\delta}$ species as active sites. *Surf. Interface Anal.* **2006**, *38*, 215−218.
(46) Chang, Q.; Zhao, K.; Chen, X.; Li, M.; Liu, J. Preparation of gold/polyaniline/multiwall carbon nanotube nanocomposites and application in ammonia gas detection. *J. Mater. Sci.* **2008**, *43*, 5861−5866.
(47) Feng, X.; Mao, C.; Yang, G.; Hou, W.; Zhu, J. J. Polyaniline/Au composite hollow spheres: Synthesis, characterization and application to the detection of dopamine. *Langmuir* **2006**, *22*, 4384−4389.
(48) Kumar, A.; Pandey, A. C.; Prakash, R. Electro-oxidation of formic acid using polyindole-SnO_2 nanocomposite. *Catal. Sci. Technol.* **2012**, *2*, 1533−2538.
(49) Pina, C. D.; Falletta, E.; Prati, L.; Rossi, M. Selective oxidation using gold. *Chem. Soc. Rev.* **2008**, *37*, 2077−2095.
(50) Manjula, P.; Boppella, R.; Manorama, S. V. A facile and green approach for the controlled synthesis of porous SnO2 nanospheres: Application as an efficient photocatalyst and an excellent gas sensing materials. *ACS Appl. Mater. Interfaces* **2012**, *4*, 6252−6260.
(51) Ahmed, M. A. K.; Fjellvag, H.; Kjekshus, A. Synthesis and characterization of tin sulphates and oxide sulphates. *Acta Chim. Scand.* **1998**, *52*, 305−311.
(52) Winjobi, O.; Zhang, Z.; Liang, C.; Li, W. Carbon nanotube supported platinum−palladium nanoparticles for formic acid oxidation. *Electrochim. Acta* **2010**, *55*, 4217−4221.
(53) Fotouhi, L.; Fatollahzadeh, M.; Heravi, M. M. Electrochemical behavior and voltammetric determination of sulfaguanidine at a glassy carbon electrode modified with a multi-walled carbon nanotube. *Int. J. Electrochem. Sci.* **2012**, *7*, 3919−3928.
(54) Danaee, I.; Jafarian, M.; Mirzapoor, A.; Gobal, F.; Mahjani, M. G. Electro-oxidation of methanol on Ni-Mn alloy modified graphite electrode. *Electrochim. Acta* **2010**, *55*, 2093−2100.
(55) Kumar, A.; Prakash, R. Synthesis of nano ground nutshell-like polyindole by supramolecular assembled salts of ss-DNA assisted chloroauric acid. *Chem. Phys. Lett.* **2011**, *511*, 77−81.
(56) Cheng, Y.; Zhang, H.; Lai, Q.; Li, X.; Shi, D.; Zhang, L. A high power density single flow zinc-nickel battery with three dimensional porous negative electrode. *J. Power Sources* **2013**, *241*, 196−202.
(57) Chen, Q.; Ai, S.; Ma, Q.; Yin, H. Selective determination of dopamine in the presence of ascorbic acid using ferrrocenyl-tethered PAMAM dendrimers modified glassy carbon electrode. *J. Appl. Electrochem.* **2010**, *40*, 1379−1385.
(58) Masarapu, C.; Zeng, H. F.; Hung, K. H.; Wei, B. Effect of temperature on the capacitance of carbon nanotube supercapacitors. *ACS Nano* **2009**, *3*, 2199−2206.
(59) Abidian, M. R.; Martin, D. C. Experimental and theoretical characterization of implantable neural mocroelectrodes modified with conducting polymer nano tubes. *Biomaterials* **2008**, *29*, 1273−1283.
(60) Ates, M.; Sarac, A. S. Electrochemical impedance spectroscopy of poly[carbazole-co-N-p-tolylsulfonyl pyrrole] on carbon fiber microelectrodes, equivalent circuits for modeling. *Prog. Org. Coat.* **2009**, *65*, 281−287.
(61) Xu, C.; Wang, L.; Mu, X.; Ding, Y. Nanoporous Pt/Ru alloys for electrocatalysis. *Langmuir* **2010**, *26*, 7437−7443.
(62) Du, B. C.; Tong, Y. Y. A coverage-dependent study of Pt spontaneously deposited onto Au and Ru surfaces: Direct experimental evidence of the ensemble effect for methanol electro-oxidation on Pt. *J. Phys. Chem. B* **2005**, *109*, 17775−17780.